Developmental Biology 344 (2010) 857–868

Contents lists available at ScienceDirect

Developmental Biology

journal homepage: www.elsevier.com/developmentalbiology

Spatiotemporally restricted regulation of generic motor neuron programs by miR-196-mediated repression of Hoxb8

Naisana S. Asli [1], Michael Kessel *

Research Group Developmental Biology, Department of Molecular Cell Biology, Max Planck Institute for Biophysical Chemistry, Am Fassberg 11, Göttingen 37077, Germany

ARTICLE INFO

Article history:
Received for publication 8 January 2010
Revised 29 May 2010
Accepted 1 June 2010
Available online 8 June 2010

Keywords:
MicroRNAs
Hox genes
Motor neuron generation
Cell cycle

ABSTRACT

Hox transcription factors are key determinants of antero-posterior identity and have been implicated in assigning positionally appropriate neuron subtypes in the neural tube. These roles inherently necessitate stringent control mechanisms that confine Hox protein activities to discrete spatiotemporal domains. Here, we provide evidence that the timing and rostro-caudal extent of Hoxb8 activity in the neural tube is tightly regulated by miR-196, a microRNA species encoded within three Hox gene clusters. In vitro and in vivo sensor-tracer analysis and transcription assays revealed that miR-196 activity restricts the caudal extent of Hoxb8 expression to the thoracic-lumbar intersect via 3' UTR-dependent negative regulation. Spatio-temporally inappropriate Hoxb8 activity, through relief of miR-196-mediated repression or direct misexpression, affected normal progression of motor neuron genesis by affecting generic motor neuron differentiation programs. In addition to uncovering a role for microRNA-dependent restriction of caudal Hox activities, these data thus indicate novel aspects of Hox-dependent neural tube patterning by revealing a requirement of temporal regulation of a generic neuronal specification program.

Introduction

The assembly of functional CNS circuits entails the acquisition of neuronal phenotypes in register with specific positions along the body axis (Edlund and Jessell, 1999; Sur and Rubenstein, 2005). This is particularly well illustrated in the developing spinal cord of the chick where motor neurons (MN) become organized into discrete columnar and pool clusters, in sync with unique axon targeting preferences for select muscle targets along the body axis (Landmesser, 2001; Tanabe and Jessell, 1996). Throughout the rostro-caudal extent of the nascent spinal cord, a gradient of Sonic hedgehog (Shh) protein, secreted from the floor plate, results in the ventro-lateral subdivision of the mitotic progenitor cells into discrete progenitor domains. Certain Shh threshold levels within the ventral neural tube result in the establishment of the MN progenitor (pMN) domain defined by co-expression of Homeodomain (HD) proteins, Nkx6.1 and Pax6, with Nkx2.2 and Irx3 which limit its ventral and dorsal boundaries, respectively (Dessaud et al., 2008; Jessell, 2000; Lee and Pfaff, 2001; Price and Briscoe, 2004). The activity of Nkx6.1/Pax6 within this MN progenitor domain is thought to activate expression of the basic Helix-loop-helix (bHLH) transcription factor Olig2. Olig2 in turn represents a key node in the MN differentiation process, by linking overall neurogenic differentiation programs with the acquisition of a generic MN identity (Marquardt and Pfaff, 2001; Mizuguchi et al., 2001; Novitch et al., 2001; Rowitch et al., 2002). The transient activity of Olig2 within subsets of pMN drives the further progression of MN specification by activating expression of MNR2 and Lim3 LIM-HD MN determinants, as well as neurogenic bHLH proteins, such as Ngn2. It also serves to suppress precocious activation of postmitotic MN markers and gliogenic factors (Lee et al., 2005; Novitch et al., 2001; Tanabe et al., 1998; William et al., 2003). Activation of MNR2/Lim3/Ngn2 just prior to cell cycle exit eventually results in the activation of the LIM-HD proteins Isl1, Isl2 and Hb9, and the consolidation of postmitotic MN identity (Jessell, 2000). Concomitant with postmitotic specification, MNs further diversify into distinct columnar and pool identities in register with their antero-posterior locale. At limb levels, MNs cluster into medial and lateral motor columns (MMC and LMC), sending axons to axial and limb muscles, respectively (Jessell, 2000; Landmesser, 2001).

Hox proteins appear to play a central role in assigning discrete columnar identities with respect to their rostro-caudal position (Dasen et al., 2003, 2005; Kessel, 1994). In higher vertebrates, the 39 Hox genes map to four distinct paralogous clusters, named Hoxa to Hoxd, which exhibit temporal and spatial collinearity (Duboule, 2007; Duboule and Dolle, 1989; Gaunt, 1988; Iimura and Pourquie, 2007; Pearson et al., 2005); genes located more 3' in a cluster are expressed earlier and more rostrally than 5' genes, which are expressed later and more caudally. This collinearity is to a large extent preserved in the spinal cord, resulting in distinctly overlapping expression domains that confer unique combinations of Hox proteins to different rostro-caudally positioned MNs.

* Corresponding author. Fax: +49 5512011504.
E-mail address: mkessel1@gwdg.de (M. Kessel).
[1] Present address: Department of Developmental Biology, Victor Chang Cardiac Research Institute, 405 Liverpool Street, Darlinghurst, NSW 2010, Australia.

0012-1606/$ – see front matter © 2010 Elsevier Inc. All rights reserved.
doi:10.1016/j.ydbio.2010.06.003

This exceptional spatiotemporal coordination implies tight regulatory mechanisms that confine individual Hox proteins to specific domains. Recently, post-transcriptional regulation through specific noncoding RNAs has been implicated in aiding this process, by repressing transient spatio-temporally inappropriate Hox expression domains (Rinn et al., 2007; Sessa et al., 2007). The repressive effect of microRNAs (miR) is exerted via direct binding to their target sequences in the 3' untranslated region (3'UTR) of an mRNA. The degree/level of repression is further determined by the complementarity of the miR-mRNA sequences, resulting in translational repression or mRNA degradation, for partial or complete complementarities, respectively (Brodersen and Voinnet, 2009; Filipowicz et al., 2008; Nilsen, 2007; Pillai, 2005). miR-196 microRNAs are encoded within the Hoxa, b and c clusters, and were shown to selectively target Hoxa7, b8 and c8, based on bioinformatic and microRNA-reporter analyses (Ohler et al., 2004). Bioinformatic analyses also predicted several additional Hox genes as putative targets of miR-196 (Grimson et al., 2007; Yekta et al., 2008). Viral overexpression of miR-196 in chick embryos effectively prevents induction of Hoxb8 by retinoic acid in the developing forelimb (Hornstein et al., 2005), while antagomiR mediated knockdown of miR-196 in the chick paraxial mesoderm results in a posterior transformation of the last cervical vertebra and vertebral malformations (McGlinn et al., 2009). Furthermore, miR-196 was found to be involved in salamander tail and spinal cord patterning during regenerative processes (Sehm et al., 2009).

Although several Hox genes have been shown to play a role in columnar specification of MNs along the rostro-caudal axis (Dasen and Jessell, 2009; Dasen et al., 2003) and in motor pool identities (Dasen et al., 2005), little is known about their function during basic motor neuron generation. Here we show that in the caudal neural tube, Hoxb8 and miR-196 are expressed in mutually exclusive domains, with miR-196 limiting the caudal-most extent of Hoxb8 expression. This observation suggests a regulatory relationship between Hoxb8 and miR-196 in the neural tube. Through sensor-tracer analysis and translation/transcription assays, we show that in the chick, miR-196 acts via 3'UTR-mediated suppression of Hoxb8 translation. Experimentally disrupting the normal spatiotemporal pattern of Hoxb8, through direct misexpression or miR-196 inhibitor mediated derepression, selectively impairs normal progression of MN determination programs. This study thus provides evidence for spatiotemporal regulation of a generic neuronal specification program through microRNA-mediated confinement of Hox protein activity.

Materials and methods

Northern blot analysis, RNase protection assay, whole mount in situ hybridization

Total RNA was extracted using TRIZOL (Invitrogen). Northern hybridization for the detection of small RNAs was performed as described (Brown, 2001) using LNA (miRCURY™ mmu-miR-196-a detection probe, Exiqon) or DNA probes against miR-196 or U6 small RNAs, respectively (for sequences see Table S1). Northern detection of the chick 3'UTR was performed according to standard protocols using total RNA separated on a formalin denaturing agarose gel and detected using chick Hoxb8-3'UTR antisense RNA probe (Sequence in Table S1). Reverse Transcriptase (RT) semi-quantitative PCR was performed on embryonic total RNA using the primers listed in Table S1, and the Qiagen One-step RT-PCR kit following manufacturer's instructions. Detection of miR-196 by RNase protection assay was performed using the miRVANA™ microRNA detection kit (Ambion) following manufacturer's instructions. For probe sequences refer to Table S1. Chicken embryos were staged as Hamburger and Hamilton (HH) stages (Hamburger and Hamilton, 1951), and mouse embryos according to days after fertilization plugs (dpc—days post-coitum). Whole mount in situ hybridization was performed using DIG-labeled probes, mapping to nucleotides 302–632 of the chick Hoxb8 mRNA (NM_204911) and nucleotides 1214–1531 of the mouse Hoxb8 mRNA (NM_010461). Whole mount in situ hybridization for the miR-196 was performed as described before (Kloosterman et al., 2006) using miR-196 LNA probe (Exiqon; for sequence see Table S1).

Western blot analysis, immunohistochemistry, BrdU labeling

Western blot analysis was performed on total protein extracts, run on a 10% SDS gel and blotted to nitrocellulose membrane. The following antibodies/dilutions were used: Hoxb8 (mouse, Abnova/1:1000), GFP (mouse, Roche/1:1000), alpha tubulin (mouse, Sigma/1:4000), H2B (rabbit, Upstate/1:2000). Immunostaining was performed as described previously (Sharma et al., 1998). Unless otherwise indicated, transverse (10 μm) or horizontal (100 μm) cryosections were analyzed. The antibodies/dilutions used were as follows: Hoxb8 (mouse, Abnova/1:100), Olig2 (rabbit, Abcam/1:500), dsRED (rabbit, Clontech/1:500), H3P (mouse, CST/1:100), GFP (mouse, Roche/1:500), GFP-Alexafluor488 conjugated (rabbit, Invitrogen/1:1000), p27kip1 (mouse, Abcam/1:500). The Isl1/2 (39.4D5), Isl2(51.4H9), Lim1/2(4F2), Nkx2.2(74.5A5), Nkx6.1 (F55A10), Pax6, Pax7 and MNR2(81.5C10) antibodies were obtained from the developmental studies hybridoma bank, under the auspices of the NICHD and maintained by the University of Iowa, Department of Biological Sciences. For BrdU labeling, the embryos were incubated with a 100 μM BrdU (Sigma) solution for 30 min. The immunostaining was performed with GFP-Alexafluor488 conjugated (rabbit, Invitrogen/1:1000) and BrdU (mouse, Roche/1:50) antibodies.

Vector details, cell culture/ transfection methods, microscopy

For all vector maps see Fig. S1. The miR-196 expression vector was generated by cloning a genomic DNA fragment of 675 bp flanking the miR-196 hairpin into the *Mlu*I and *Nhe*I sites of the bicistronic vector described previously (Das et al., 2006). The pCAGGS-Hoxb8 expression vector was created by cloning the chick Hoxb8 coding sequence (NM_204911) into the *Eco*RI site of the pCAGGS vector (For primer sequences see Table S1). The Hoxb8-IRES-GFP vector was generated by subcloning the Hoxb8 frame from the pCAGGS-Hoxb8 into the *Eco*RI sites of the pMX-IRES-GFP vector. The CMV-GFP-sensor and CMV-GFP-B8UTR vectors were generated by annealing designed oligonucleotides (Table S1) and their subsequent cloning into the *Hin*dIII and *Bam*HI sites of the CMV-EGFP-C1 vector (Clontech). To generate the luciferase sensor, the annealed oligonucleotides were cloned into the *Xho*I and *Not*I sites of the psiCheck double luciferase vector (Promega; for sequence see Table S1). For the miR-196 knockdown the miRIDIAN miR-196 inhibitor was used and as the negative control miRIDIAN microRNA negative control 2 RNA oligonucleotides (Dharmacon) were used, both as 200 pmol stocks in 1× siRNA buffer (Dharmacon). The inhibitor molecules were hairpin RNA oligonucleotides with chemical enhancements to improve efficiency and longevity. The cell lines used include human HEK293T and chick embryonic fibroblast (CEF) cells. HEK293T cells were transfected by FuGENE6 (Roche) and CEF cells by Lipofectamine™ 2000 (Invitrogen), following the manufacturer's instructions. All image analyses were performed on an Olympus BX60 fluorescence microscope or a Leica TCM laser scanning microscope.

Luciferase assay, quantitations, statistical analysis

The luciferase assay was performed using the Dual-luciferase reporter assay kit (Promega) on the Victor™Light 1420 luminescence counter (Perkin Elmer) and relative luciferase activity determined as Renilla/Firefly luciferase values. For quantitation of immunostained sections, the number of cells positive for each marker was counted in the electroporated and the contra-lateral non-electroporated side of the neural tube. The ratios of electroporated:non-electroporated cell

numbers were then averaged between six successive sections. The same calculations were done in control (e.g. GFP-electroporated) embryos and the values compared as block diagrams between the experimental and control embryos. The significance of the differences was determined by the paired Student *t*-test (Excel-Microsoft). Quantitation of western blot signal was performed using ImageJ (Girish and Vijayalakshmi, 2004), normalizing the absolute intensities to the H2B loading control.

Electroporation, retrograde labeling

DNA solutions were injected into the neural tube in concentrations of 0.7–2.0 μg/μl, and electroporation performed as previously described (Krull, 2004), with 5 pulses of 25 volts, 50 ms each with 950 ms intervals, using Electro Square Porator ECM830 (BTX). Retrograde axonal labeling was performed using Alexa594-conjugated Dextran (Invitrogen) as previously described (Glover et al., 1986). In summary the dextran dye was applied to the base of the hindlimb in E5 embryos. The embryos were kept for 4–5 h in carbogenated Tyrode's buffer for proper labeling of the LMC columns and then fixed, embedded in cryomatrix, sectioned horizontally (100 μm), and processed for immunostaining.

Results

miR-196 and Hoxb8 are expressed in mutually exclusive domains along the antero-posterior neuraxis

During early neural development in chick, Hoxb8 is expressed in a highly dynamic fashion in the neural tube. Initially, at stage HH13, its expression extends from an anterior boundary at somites 6–7 to the caudal end of the embryo, including the open neural folds and the flanking presomitic mesoderm at the prospective hindlimb level (Bel-Vialar et al., 2002 ; Fig. 1A). At HH15-16, Hoxb8 expression is extinguished from the caudal-most neural tube posterior to somites 23–24, the prospective hindlimb field (HLF), while retaining the early anterior boundary at somites 6–7 (Fig. 1B).

Previous data implicated microRNA miR-196 as a negative regulator of Hoxb8 activity. We therefore investigated the expression of miR-196 at axial levels posterior to somites 23–24. At HH13, where the expression of Hoxb8 continues in the HLF region, no miR-196 was detected (Fig. 1A). However, miRNA detection in total RNA derived from three different axial levels of HH15 embryos, revealed exclusive expression of miR-196 at levels posterior to somites 23–24 (Fig. 1B). Similarly, whole mount in situ hybridization on 9.5 days postcoitum (dpc) mouse embryos, using a DIG-labeled miR-196 LNA probe, demonstrated a posteriorly restricted miR-196 expression domain, complementary to, and mutually exclusive with Hoxb8 (Fig. 1C). These observations suggested that miR-196 activity is confined to a caudal neural tube domain excluded by Hoxb8 expression. To further investigate this, we designed a fluorescent sensor reporter (CMV-GFP-sensor) based on a cassette encoding green fluorescent protein (GFP), followed by a direct repeat of perfect miR-196 complementary sites (Fig. S1). The presence of such complementary sites is predicted to render sensor mRNAs degradable by matching miRNAs (Mansfield et al., 2004). Indeed, in transfected chick embryonic fibroblasts (CEFs) expressing basal levels of miR-196 (Fig. S2A), GFP expression driven by CMV-GFP-sensor was selectively suppressed, while control vector CMV-GFP showed normal expression (Fig. S2B and S2C).

We next addressed the distribution of endogenous miR-196 activity in vivo upon introducing the CMV-GFP-sensor into the neural tube of HH14 embryos via in ovo electroporation. At all subsequent steps, transfection efficacy was monitored by the co-introduction of the non-regulated tracer plasmid CMV-dsRED (Fig. 1D and S1). Co-transfection of CMV-dsRED-tracer together with control CMV-GFP vector lacking miR-196 target sites resulted in extensive dsRED and GFP co-expression along the entire rostro-caudal axis of the neural tube (Fig. 1D). In contrast, GFP driven by CMV-GFP-sensor was always found to be excluded from the caudal-most domain of the neural tube, while dsRED derived from co-transfected CMV-dsRED-tracer concomitantly showed unbiased expression throughout this domain (Fig. 1D). Taken together, these data indicate that the caudal-most Hoxb8-negative domain of the neural tube is an endogenous source of repressive miR-196 activity.

miR-196 effectively suppresses endogenous Hoxb8

Our observations suggest that miR-196 may be involved in negative regulation of Hoxb8 activity within the neural tube. We therefore decided to test the impact of ectopic miR-196 on endogenous Hoxb8 expression in vivo. To achieve effective exogenous miR-196 expression, we generated a bicistronic vector (Ac-dsRED-miR196), encoding dsRED driven by the actin (Ac) promoter, and miR-196 driven by U6 promoter (Fig. S1). Upon transfection in HEK293T cells, Ac-dsRED-miR196, but not Ac-dsRED control vector, generated substantial amounts of miR-196, and effectively reduced the activity driven by co-transfected luciferase reporters carrying two perfect miR-196 complementary sites (Fig. S3A and S3B). In order to analyze the activity of ectopic miR-196 in vivo, Ac-dsRED-miR196 and Ac-dsRED control vector were separately electroporated into the HH14 neural tube, followed by analysis of the impact on endogenous Hoxb8 protein levels 48 h post-electroporation (HH22). Unilateral electroporation of Ac-dsRED-miR-196 into the neural tube led to ectopic expression of miR-196 as shown in northern analysis of dissected tube segments (Fig. S3C). Subsequently, dsRED-miR-196 electroporated neural tubes showed a significant decrease (35%, *p*-value = 0.0014) of Hoxb8$^+$ cells in the transfected, compared to the non-transfected side or neural tubes electroporated with Ac-dsRED control vector (Fig. 2A and B). The effect on Hoxb8$^+$ cells was independent of a change in the number of post-mitotic interneurons as depicted by the number of dorsal Lim1/2$^+$ cells (Fig. 2A and B). Thus, miR-196 effectively suppresses endogenous Hoxb8 expression in vivo, presumably by acting via predicted miR-196 target sites in the 3'UTR of the chick Hoxb8 mRNA. To further study the repressive effect of miR-196 on chick Hoxb8, we used chick embryonic fibroblast (CEF) primary cells that express basal levels of both Hoxb8 and miR-196 (Fig. 2 and S2). The same 3'UTR sequence of chick Hoxb8 was detected in total RNA from different embryonic stages as in the CEF cells (Fig. 2C), proving the CEF cells are an appropriate in vitro system to study the miR-Hox regulation. Transfection of a GFP reporter bearing the native chick Hoxb8 3'UTR into the CEFs diminished GFP expression (Fig. 2D). Ectopic expression of miR-196 by transfection of Ac-dsRED-miR196 vector into the CEF cells also resulted in a significant decrease of the endogenous Hoxb8 protein (Fig. 2E) suggesting a repressive effect of miR-196 on Hoxb8 perhaps through an effect on its 3'UTR.

Based on these observations, inhibition of miR196 was predicted to result in derepression of Hoxb8 in cells endogenously expressing low levels of both Hoxb8 and miR196. In order to test this, CEFs were transfected with either a selective inhibitor oligonucleotide against miR-196 (miR-196-inhibitor), or with a non-matching control oligonucleotide. Suppression of endogenous miR-196 resulted in a concomitant 1.8 fold ($n = 3$; *p*-value = 0.03) increase of endogenous Hoxb8 protein levels, normalized to Histone 2B (H2B; Fig. 2F). Taken together, these data suggest that miR-196 has the regulatory potential to keep the caudal-most neural tube devoid of Hoxb8 activity.

The early phase of Hoxb8 expression coincides with early motor neuron generation

The mutually exclusive expression domains of miR-196 and Hoxb8 at HH15 suggested a possible link between the two at the time when MN progenitors become specified and begin to differentiate. We therefore

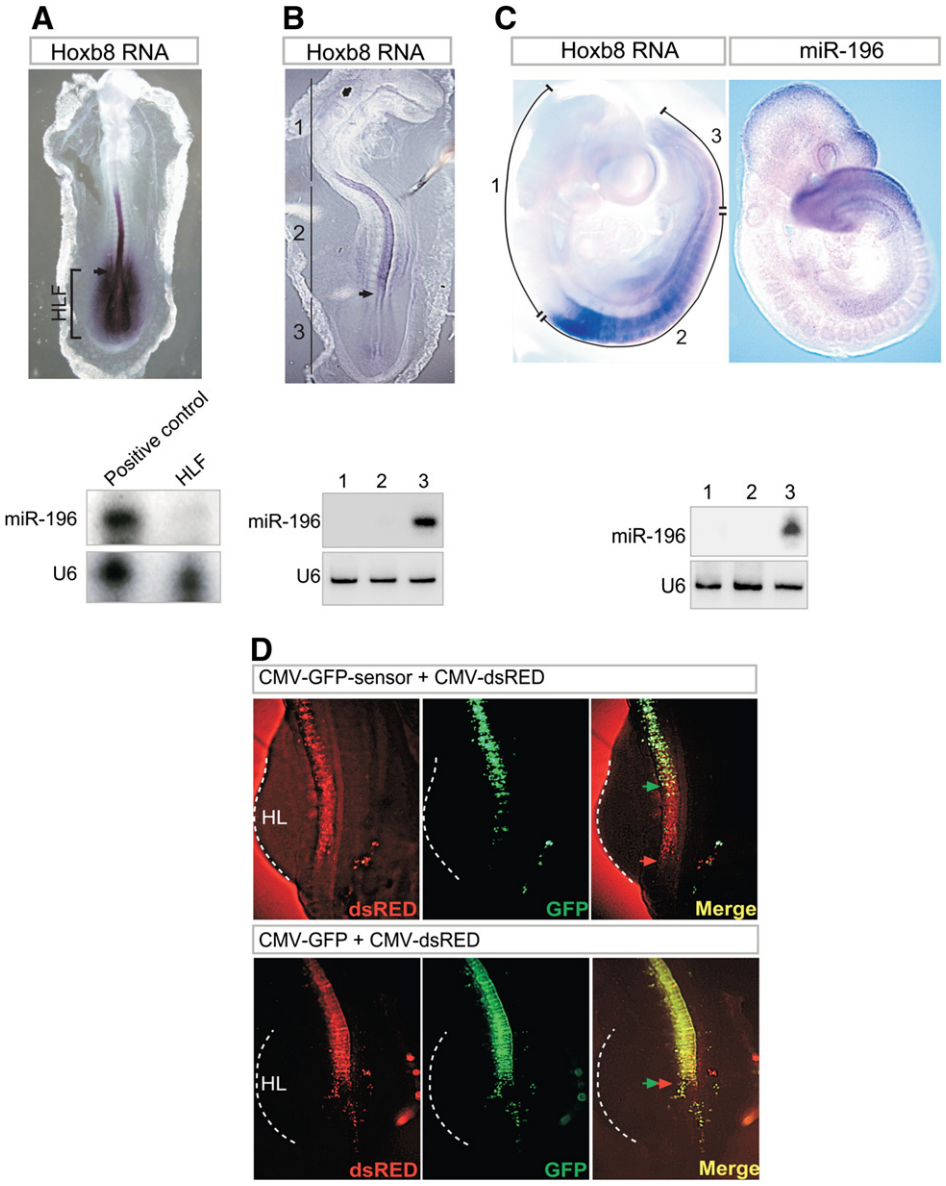

Fig. 1. Hoxb8 and miR-196 activities settle into mutually exclusive domains along the antero-posterior axis. (A) The expression of Hoxb8 and miR-196 in HH13 chick embryo. Upper panel: note the expression of Hoxb8 in the prospective hindlimb field (HLF). Lower panel: RNase protection assay shows no expression of miR-196 in the HH13 HLF. (B) The expression of Hoxb8 and miR-196 in HH15 chick embryo. Upper panel: note the absence of Hoxb8 expression in the caudal-most neural tube posterior to somites 23/24 (designated: region 3), corresponding to the future hindlimb field. Lower panel: northern blot analysis exclusively detects miR-196 in RNA extracted from region 3, but not in more rostral (regions 1, 2) neural tube segments. (Arrows in A and B point to corresponding axial regions in HH13 and HH15 embryos). (C) Upper panel: 9.5 dpc mouse embryo after whole mount in situ hybridization with DIG labeled Hoxb8 RNA antisense probe, or DIG labeled LNA probe against miR-196. miR-196 is detected in region 3, excluded by Hoxb8 expression. Lower panel: northern blot analysis detects miR-196 in RNA extracted from region 3 of 9.5 dpc mouse embryos, but not in more rostral (regions 1, 2) neural tube segments. (D) In vivo detection of miR-196 activity in post-HH15 chick neural tube through sensor/tracer analysis (see text for details). Co-localization of GFP and dsRED (yellow fluorescence) indicates the absence of suppressive activity mediated through miR-196 target sites in CMV-GFP-sensor. Note: effective exclusion of GFP, but not dsRed from region 3 neural tube upon transfection of CMV-GFP-sensor plus CMV-dsRed lacking the sensor module. Transfection of control CMV-GFP plus CMV-dsRed results in unbiased expression of both, GFP and dsRED throughout the neural tube, including region 3. Green and Red arrows indicate the posterior boundary of GFP and dsRED proteins, respectively (HL: Hindlimb).

looked at the dorso-ventral (D/V) dynamics of Hoxb8 expression in our key stage (HH15) and in later stages (HH18 and HH22), correlating Hox expression to that of the progenitor motor neuron marker, Olig2. The expression of Hoxb8 falls into two distinct patterns along the dorso-ventral neuraxis, here referred to as early and late phases of expression. During the early phase, Hoxb8 is evenly expressed along the D/V axis of the brachial neural tube, and is coexpressed with Olig2 in the motor neuron precursor domain in the ventral neural tube (Fig. 3A). The lack of Hoxb8 expression in the lumbar neural tube however, precedes the emergence of Olig2^{+} precursor MNs that finally form by HH18 (Fig. 3A). During the late phase, Hoxb8 expression becomes restricted to post-mitotic interneurons, and is completely absent from the motor neuron precursor domain and motor columns, irrespective of antero-posterior locale (Fig. 3B).

Spatiotemporally inappropriate Hoxb8 suppresses motor neuron generation

What is the significance of the tight, spatially confined regulation of Hoxb8 activity in the caudal neural tube? To address this, we manipulated spatiotemporal Hoxb8 levels and studied the impact on neurogenesis in the caudal neural tube during the early phase of Hoxb8 expression (Fig. 3A). Since the temporal downregulation of endogenous Hoxb8

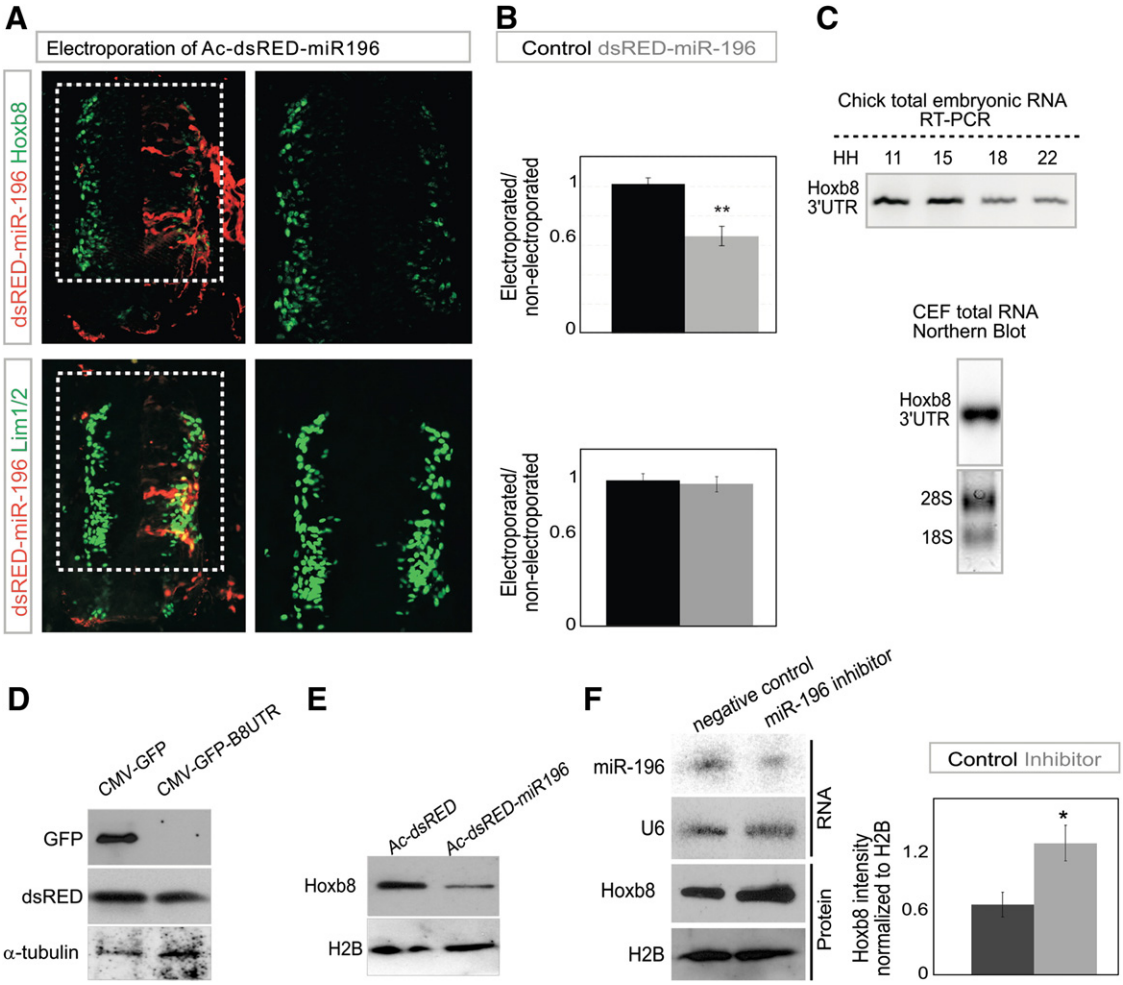

Fig. 2. miR-196 represses Hoxb8 by targeting its 3'UTR. (A) Unilateral electroporation of Ac-dsRED-miR196 into the chick neural tube results in a decrease in the number of Hoxb8$^+$ cells in the electroporated, compared to the non-electroporated side ($n=3$). Note no change in the number of Lim1/2$^+$ interneurons in Ac-dsRED-miR196 electroporated embryos. (B) Quantitation of Hoxb8$^+$ and Lim1/2$^+$ interneurons in Ac-dsRED-miR196 electroporated embryos, compared to control embryos electroporated with Ac-dsRED. (C) Upper panel: detection of identical 3'UTR sequences in the total RNA from different chick embryonic stages by RT-PCR using primers flanking the miR-196 target site in the 3'UTR region. Lower panel: same sequence of embryonic Hoxb8 3'UTR is detected by northern blot on the total RNA from chick embryonic fibroblasts (CEFs). Ribosomal RNAs (28S and 18S) are used as a measure of total RNA. (D) Decrease of GFP protein driven in CMV-GFP-B8UTR transfected CEFs compared to CMV-GFP control transfected cells. Note: no difference in the levels of co-transfected dsRED, or endogenous. α-tubulin. (E) Transfection of Ac-dsRED-miR196, but not Ac-dsRED control vector triggers reduced endogenous Hoxb8 protein levels in CEFs. (F) Inhibition of miR-196 results in 1.8 fold increase in endogenous Hoxb8 protein in CEFs, compared to negative control oligonucleotide. Hoxb8 levels were normalized to H2B levels ($n=3$, p-value = 0.03).

occurred just prior to the generation of MNs, we addressed the impact of sustained Hoxb8 expression on MN genesis in the lumbosacral neural tube. Upon electroporation into the HH14 caudal neural tube, ectopic Hoxb8 resulted in a marked reduction of MNs, as indicated by the significant decrease in the number of cells expressing the postmitotic MN markers Isl1/2 (40%; p-value = 0,0014), Isl2 (40%, p-value = 0,0054), and Lim1 (60%, p-value = 0,0054) in the HH22 ventro-lateral neural tube (Fig. 4A and B). In contrast to Isl1/2$^+$Lim1$^+$Isl2$^+$ MNs, ectopic Hoxb8 did not result in a reduction of Lim1/2$^+$Isl2$^-$ neurons in the dorsal neural tube (Fig. 4C and D). Moreover, upon Hoxb8 electroporation, no significant impact on the number of cells expressing the exclusive interneuron marker Pax2 was observed (data not shown). Thus, ectopic Hoxb8 selectively impacted MNs, but not the early generation of interneurons. These data were consistent with a requirement for Hoxb8 downregulation for commencement of normal MN genesis in the caudal neural tube.

We next asked whether Hoxb8-mediated suppression of MNs was regionally restricted, thereby reflecting its selective exclusion from the lumbosacral neural tube. To address this, we tested the impact of forced Hoxb8 expression on neuronal fates at more rostral spinal levels. Forced Hoxb8 expression resulted in no change in the number of post-mitotic MNs as depicted by Isl1/2$^+$ cells, 48 h post-electroporation in the HH22 brachial neural tube (Fig. S4). This therefore indicated a selective repressive effect of mis-expressed Hoxb8 in the generation of lumbar MNs.

Hoxb8 selectively impacts intermediate steps of motor neuron generation

How does deregulation of Hoxb8 impact generation of postmitotic MNs? Upon expression of exogenous Hoxb8, downregulation of postmitotic MN markers was accompanied by a significant increase in Olig2$^+$ cells (80%, p-value = 0,0088; Fig. 5A and B), which is normally associated with MN and oligodendrocyte progenitor cells (Novitch et al., 2001). Transient expression of the bHLH transcription factor Olig2 is normally thought to coordinate neurogenic and MN specification programs, downstream of combinatorially acting Nkx6.1 and Pax6 transcription factors (Novitch et al., 2001). Interestingly, the increase in Olig2$^+$ pMNs was not accompanied by altered expression of Nkx6.1 or Pax6 (Fig. S6A). Similarly, no alteration in the expression of inherent markers of progenitor domains bordering the pMN domain (Pax7, Nkx2.2) could be detected upon forced Hoxb8 expression (Fig. S6B).

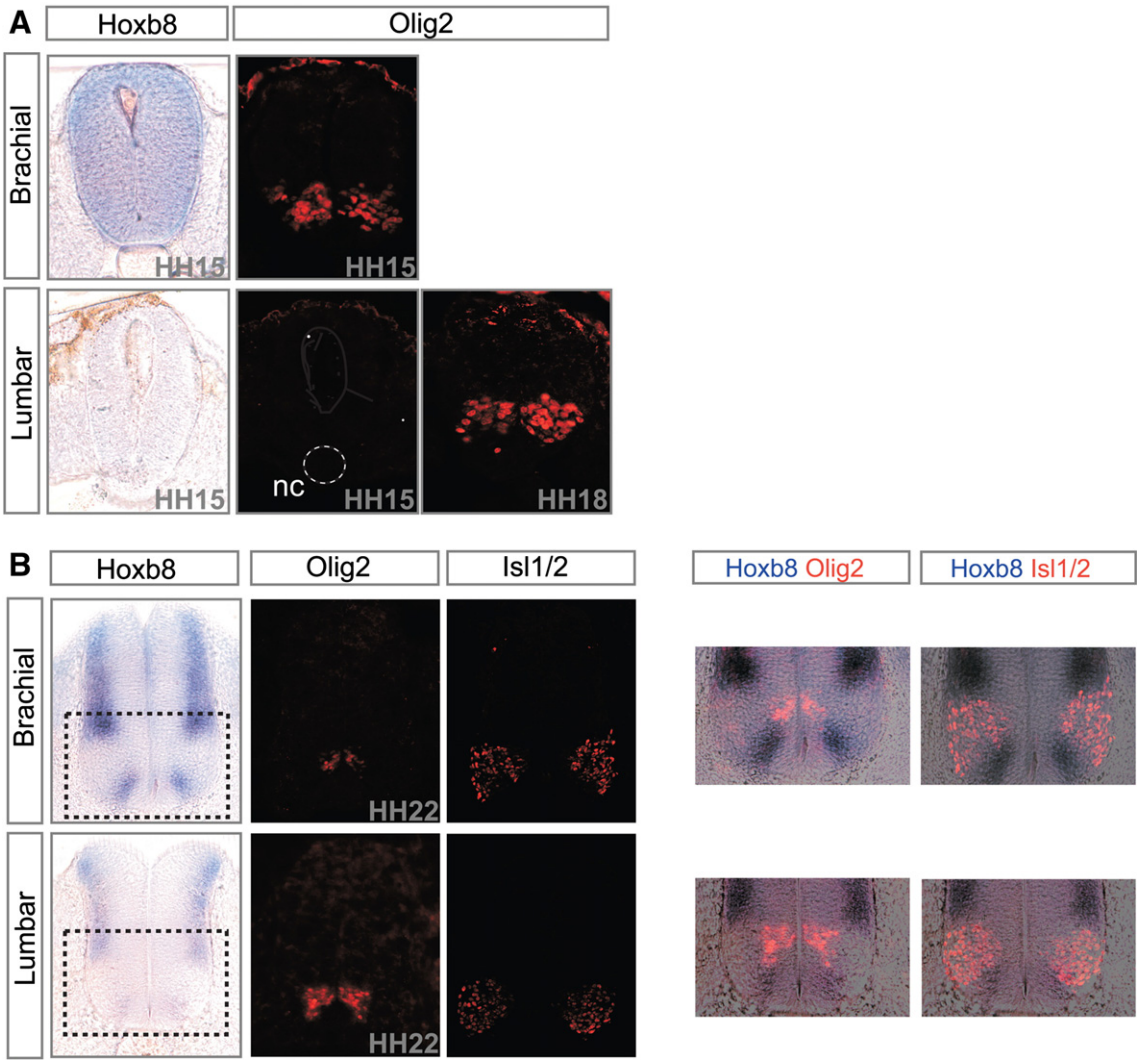

Fig. 3. Hoxb8 is expressed in a distinct dorso-ventral pattern during motor neuron generation. (A) During the early phase, Hoxb8 is evenly expressed along the dorso-ventral axis of the HH15 brachial neural tube, whereas expression is absent in the lumbar neural tube. Note the co-expression of Hoxb8 and the progenitor motor neuron marker, Olig2 during the early stage. In the lumbar neural tube, lack of Hoxb8 precedes the generation of progenitor MNs at HH18. nc: notochord. (B) During the late phase (HH22), Hoxb8 expression is restricted to the post-mitotic interneurons leaving the motor neuron domain Hoxb8 negative. Note the exclusive expression domains of Hoxb8 and, Olig2, the marker for motor neuron precursors, and Isl1/2, the marker for postmitotic MNs in the merged figures on the right.

Thus, Hoxb8 appears to selectively act during a transient phase in MN genesis, prior to the commitment of postmitotic MN fates but following the early determination of MN progenitor identity.

To further investigate this, we decided to more narrowly define the window of Hoxb8 action on MN differentiation. During MN generation, the transcription factor MNR2 is thought to be activated downstream of Olig2, prior to terminal cell cycle exit and upregulation of Isl1/2 (Tanabe et al., 1998). Misexpression of Hoxb8 resulted in a significant decrease (40%, p-value = 0.015) in the number of MNR2$^+$ MNs (Fig. 5A and B). To investigate whether this is reflected by selective impacts on cell cycle progression, we next determined the number of cells in S phase by administration of a 30-min BrdU pulse in Hoxb8 and control electroporated embryos. Hoxb8 expression resulted in a significant increase in the number of BrdU$^+$ cells (20%, p-value = 0.021; Fig. 5A and B). At the same time, no significant impact on numbers of cells positive for the M-phase marker phospho-Histone H3 (H3P) could be detected upon Hoxb8 electroporation (Fig. S5). Taken together, these observations suggest that ectopic Hoxb8 expression affects motor neuron generation at the phase of cell cycle exit.

We next decided to test whether the failure of inherent MN marker expression (i.e. MNR2, Isl1/2, Lim1) was accompanied by defective acquisition of generic MN properties, such as postmitotic neuronal marker expression and axon extension out of the spinal cord. To address this, we first tested the expression of the cyclin dependant kinase (cdk) inhibitor, p27kip1, a hallmark of postmitotic neurons (Tarui et al., 2005). Forced Hoxb8 expression in lumbosacral neural tube resulted in a decrease in the number of p27kip1$^+$ cells (20%, p-value = 0.018; Fig. 5A and B), further suggesting that Hoxb8 could suppress terminal cell cycle exit. To address this possibility, we performed retrograde labeling of peripheral axon projections through the bilateral application of fluorescent dextran conjugates to nerve endings in the hindlimb musculature upon both control GFP and Hoxb8/GFP expression. This resulted in effective retrograde tracing of the somas of MNs within the lumbar LMC (Fig. 6). From control GFP-electroporated embryos, LMC neurons were effectively back-traced from the limb, and many GFP$^+$Dextran$^+$ MNs could be observed (Fig. 6B and C). In contrast, upon effective Hoxb8/GFP expression, a pronounced mutual exclusion of GFP$^+$ and Dextran$^+$ cells within the LMC was observed (Fig. 6A and C), indicating that many Hoxb8 expressing cells failed to successfully extend axons into the limb. Taken together, Hoxb8 appears to selectively impact late phase pMNs, resulting in prolonged maintenance of Olig2$^+$ pMN status and failure of postmitotic MN differentiation.

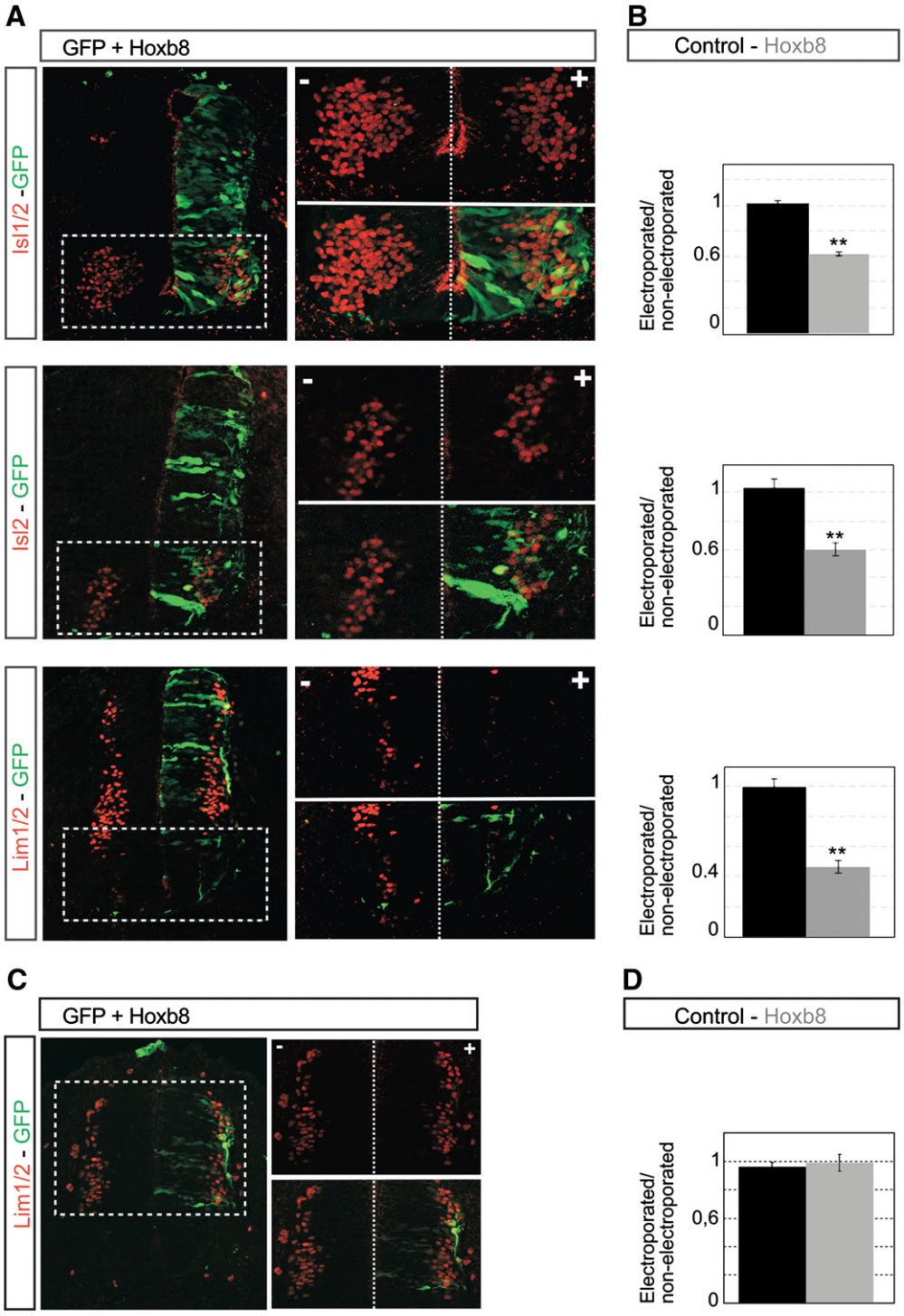

Fig. 4. Spatiotemporally inappropriate Hoxb8 suppresses motor neuron generation. (A, B) Co-electroporation of pCAGGS-Hoxb8 and CMV-GFP into HH14 chick neural tube reduces postmitotic motor neuron (MN) numbers ($n=5/5$): (A) Generation of postmitotic MNs in the HH22-25 ventro-lateral spinal cord (prospective ventral horn) was tested through immunodetection for Isl1/2, Isl2, Lim1/2. Hoxb8 results in reduction of Isl1/2$^+$, Isl2$^+$, Lim1/2$^+$ cells in the MN-containing ventral horn ("+" and "−" indicate electroporated and control sides of the neural tube, respectively). (B) Quantitative summaries of cells expressing postmitotic MN markers in the ventral horn of Hoxb8-electroporated, compared to the control embryos electroporated with CMV-GFP. (C, D) Expression of dorsal interneuron markers upon forced Hoxb8 expression: (C) Co-electroporation of pCAGGSS-Hoxb8 and CMV-GFP into HH14 chick neural tube. Note: Hoxb8 misexpression does not change the number of Lim1$^+$ cells in the dorsal neural tube ($n=3$). "+" and "−" indicate electroporated and control sides of the neural tube, respectively. (D) Quantitative summary of Lim1$^+$ cells in Hoxb8 and control electroporated embryos. Only cells of the dorsal neural tube (excluding the ventral horn) were considered for quantitations.

Selective miR-196 knockdown phenocopies Hoxb8 misexpression in repressing normal generation of lumbar motor neurons

Our data suggest that timed downregulation of Hoxb8 is required for normal progression of lumbar MN differentiation programs. Based on the effective repression of Hoxb8 activity by miR-196, we predicted that repression of endogenous miR-196 would trigger impacts on MN generation analogous to those seen upon direct Hoxb8 misexpression. To test this idea, the HH14 lumbar neural tube was electroporated with miR-196-inhibitor RNA oligonucleotides and the generation of MNs

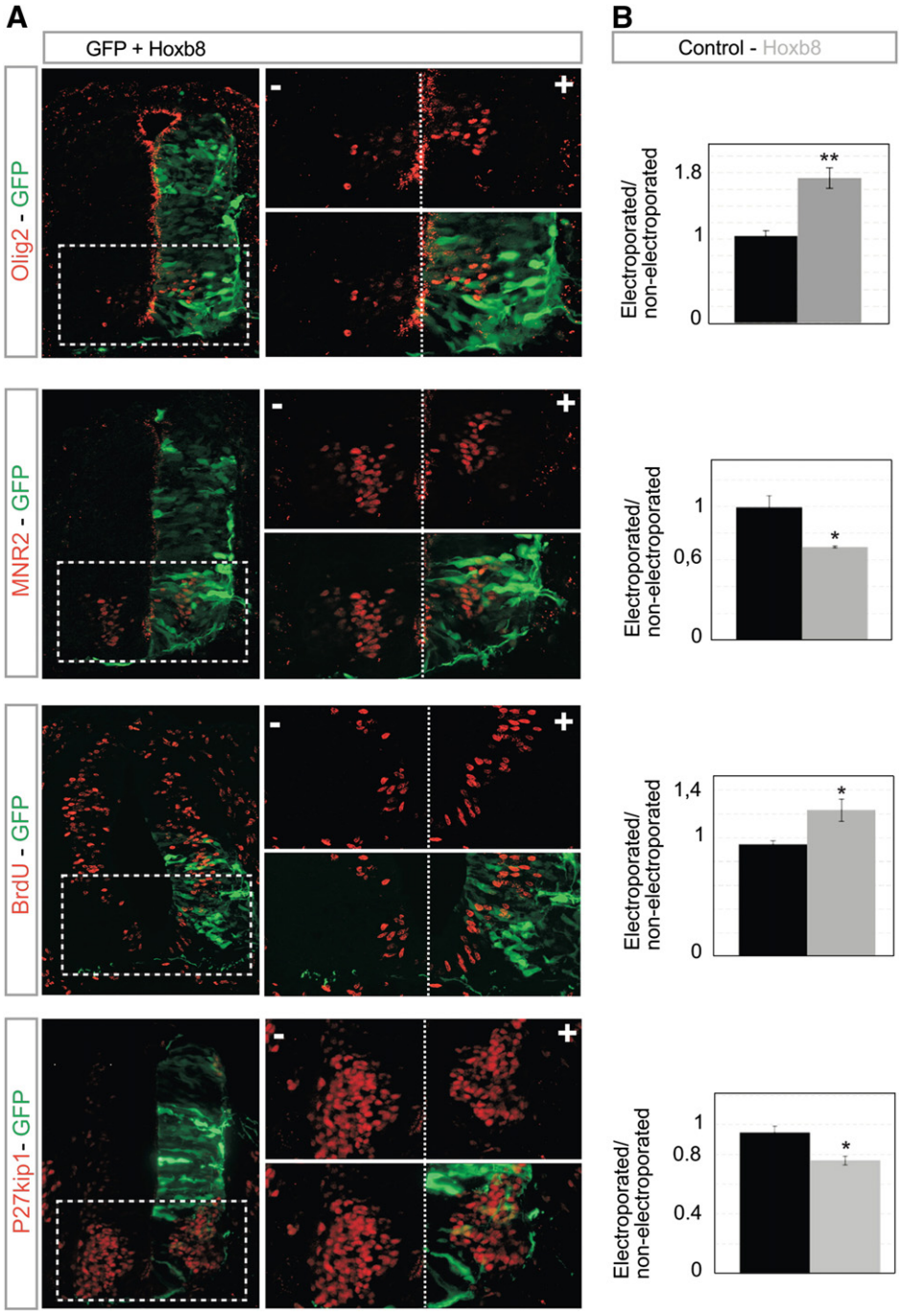

Fig. 5. Hoxb8 affects progression of motor neuron programs at intermediate progenitor stages. Co-electroporation of pCAGGS-Hoxb8 and CMV-GFP into HH14 chick neural tube ("+" and "−" indicate transfected and control sides of the neural tube, respectively). Immunodetection for indicated proteins on E4 spinal cord sections at lumbar levels. (A) In the ventral ventricular zone, Hoxb8 triggers an increase in Olig2$^+$ and BrdU$^+$ cells ($n=5$). Hoxb8 expression results in a decrease in the number of MNR2$^+$ and P27kip1$^+$ postmitotic MNs ($n=5$). (B) Quantitation of Olig2$^+$, BrdU$^+$, MNR2$^+$ and p27kip1$^+$ cell numbers in the ventro-lateral spinal cord of pCAGGS-Hoxb8, compared to CMV-GFP-electroporated control embryos.

monitored 48 h post-electroporation. Similar to direct Hoxb8 misexpression, knockdown of miR-196 resulted in a marked increase in the number of Olig2$^+$ cells (60%, p-value = 0,0074; Fig. 7A and B). Concomitantly, a significant reduction in the number of Isl1/2$^+$ MNs was observed (20%, p-value = 0,001; Fig. 7A and B). By comparison, electroporation of heterologous microRNA sequences from *Caenorhabditis elegans* with no homologue in vertebrates did not result in measurable effects on Isl1/2$^+$ and Olig2$^+$ cell numbers (Fig. 7B: quantitation plots). The effect of the miR-196 knockdown was further mirrored by a decrease of Isl2$^+$ and Lim1$^+$ post-mitotic MNs in a fraction of embryos ($n=2/6$; p-values = 0.036 and 0.019, respectively), but stayed unchanged in the rest (data not shown). The similar repressive effects of forced Hoxb8 expression and miR-196 knockdown on the generation of lumbar MNs suggest a common mechanism of action. miR-196 knockdown resulted in no detectable ectopic expression and/or upregulation of Hoxb8 protein in the lumbar motor column (data not shown), suggesting the miR-196 regulatory effect as secondary to the main transcriptional control of Hoxb8.

Several Hox mRNAs are suggested as putative targets of miR-196. Knock down of miR-196 could therefore also result in derepression of other targets leading to defective motor neuron generation. To address this question, we checked if forced expression of miR-196 and hence

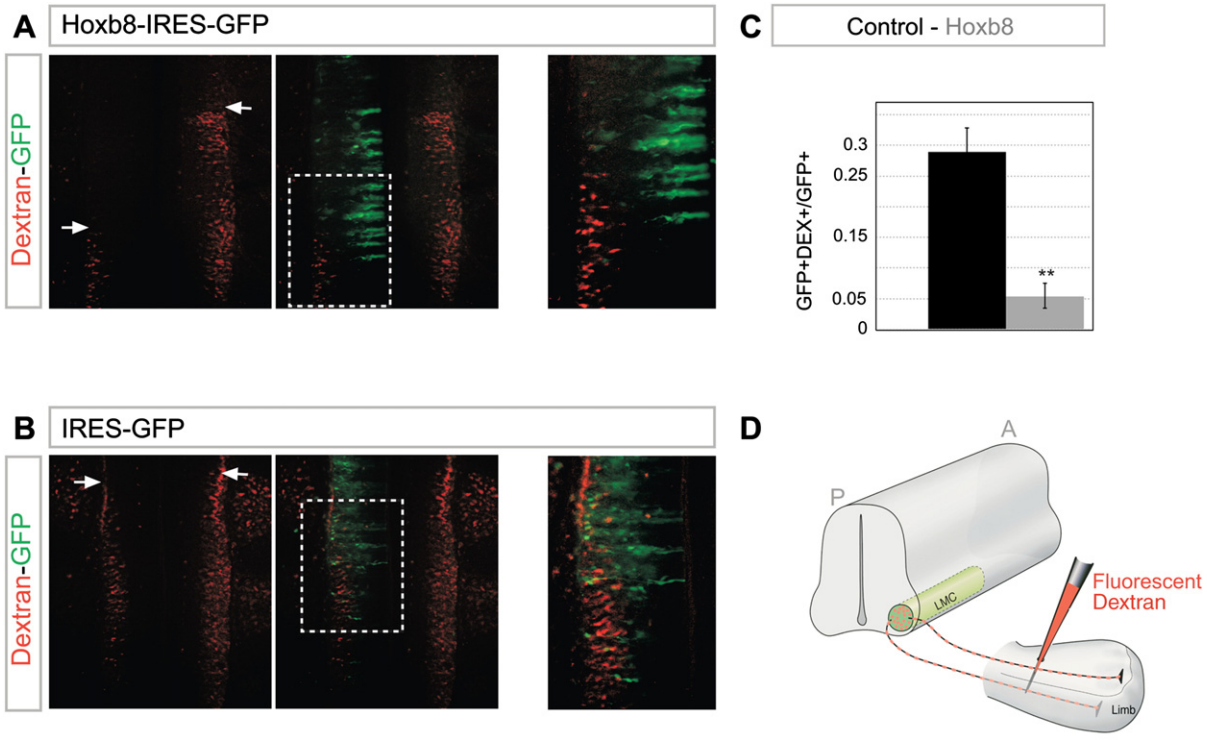

Fig. 6. Hoxb8-mediated suppression of lumbar motor axon extension. (A–B) Bilateral fluorescent-dextran-mediated retrograde tracing of hindlimb-innervating motor axons on horizontal sections of E5 embryos, after unilateral electroporation of Hoxb8-IRES-GFP (A), or the control IRES-GFP vectors (B). (A) Forced Hoxb8 expression (GFP^+ cells) leads to marked reduction of retrogradely traced $dextran^+$ MNs in the lumbar LMC ($n=5$), indicating failure of Hoxb8/GFP^+ MNs to innervate the limb. (B) Transfection of IRES-GFP control vector does not alter effectiveness of retrograde tracing of LMC neurons compared to the control side. Arrows indicate the anterior boundary of the lumbar LMC. (C) Quantitative summary of $GFP^+dextran^+$ versus total GFP^+ cell numbers shows significant reduction in the proportion of $GFP^+dextran^+$ cells upon Hoxb8-IRES-GFP transfection ($n=3$, p-value $=0.0007$). (D) Schematic diagram of retrograde dextran labeling: lumbar motor neuron projections are labeled at the base of the E5 embryonic hindlimb and labeled cell bodies are analyzed on horizontal sections. (A: Anterior, P: Posterior, LMC: Lateral Motor Column).

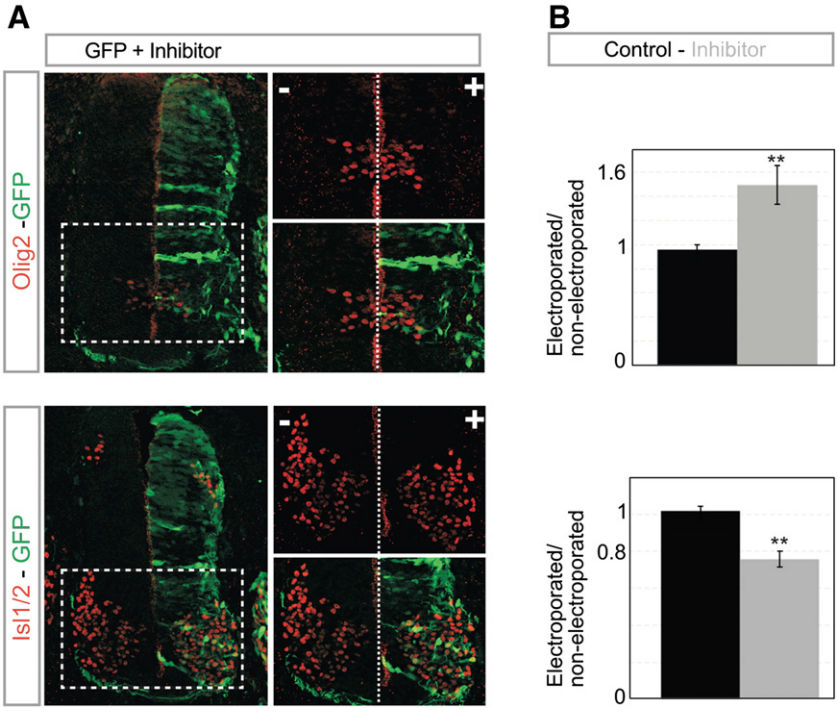

Fig. 7. Impacts of miR-196 silencing on the generation of lumbar motor neurons. Co-electroporation of miR-196-inhibitor RNA oligonucleotide plus CMV-GFP into lumbar HH14 chick neural tube phenocopies impacts of direct Hoxb8 expression on $Isl1/2^+$ MNs and $Olig2^+$ pMNs ($n=6$). (A) Unilateral transfection of miR-196-inhibitor results in an increase in $Olig2^+$ pMNs, and a concomitant decrease in $Isl1/2^+$ MNs. ("+" and "−" indicate electroporated and control sides of the neural tube, respectively). (B) Quantitation of the number of cells positive for each marker within the ventral horn of miR-196-inhibitor electroporated embryos, compared to embryos electroporated with the negative control oligonucleotide.

additional down regulation of other non-Hoxb8 putative targets could affect lumbar motor neuron generation. For this purpose, Ac-dsRED-miR196 was electroporated into the HH14 chick neural tube and lumbar motor neuron generation was studied 48 h post-electroporation (HH22). Forced expression of miR-196 in the lumbar neural tube, did not lead to any significant change in motor neuron generation as confirmed by the expression of Olig2, Isl1/2, Isl2 and Lim1 (Fig. S7). We then asked if the miR-196 mediated repression of Hoxb8 is sufficient to alter motor neuron generation/differentiation programs. To address this question, Ac-dsRED-miR196 was electroporated into the HH14 brachial neural tube and motor neuron generation was studied 48 h post-electroporation. Misexpression of miR-196 in the brachial neural tube, did not result in any significant change in motor neuron generation as observed by Olig2, Isl1/2, Isl2 and Lim1 expression (Fig. S8) suggesting that Hoxb8 down regulation per se is not sufficient to drive motor neuron generation.

Discussion

In this study, we provide evidence for a microRNA-mediated mechanism that delimits Hoxb8 activity within a concise spatio-temporal domain. Timed downregulation of Hoxb8 through miR-196 appears to assure normal progression of a generic MN differentiation program. Below, we discuss the implication of these data in light of previous results on Hox protein function and regulation during neural tube patterning and neural specification.

Hoxb8 and miR-196 in the neural tube

It is thought that in mammals, the presence of microRNA target sites in the 3'UTR of mRNAs causes an evolutionary constraint, resulting in an "avoidance mechanism" through which a microRNA and its putative targets adopt exclusive expression domains (Farh et al., 2005). Similarly, miR-196 was previously shown to display a distribution suggesting complementarity with at least some of its putative Hox target mRNAs. In mice, a LacZ-sensor transgene fused to miR-196 complementary target sites resulted in exclusion of lacZ expression in the posterior trunk at 10 dpc—a pattern mirrored by the detection of endogenous miR-196 through in situ hybridization with LNA probes (Fig. 1C) (Kloosterman et al., 2006; Mansfield et al., 2004). In the present study, we demonstrated that the neural folds of the chick hindlimb field initially express Hoxb8, but not miR196. Only when miR196 became detectable, did we observe a regression of Hoxb8 from the neural tube at the level of the hindlimb. Thus, the posterior boundary of Hoxb8 expression became defined and sharpened in the lumbar region in parallel with the formation and differentiation of the neural tube. Our attempts to influence Hoxb8 levels in this zone by miR196 reduction remained unsuccessful, for as of yet unexplained reasons. The adoption of mutually exclusive domains in the neural tube, suggests a negative regulatory function of miR-196 on Hoxb8. In addition to Hoxb8, reporter assays with several Hox 3'UTRs implicated Hoxc8 and Hoxa7 as potential targets of miR-196 (Ohler et al., 2004). However, Hoxb8 appears to be the only putative miR-196 Hox target showing complementary mRNA expression in HH15/16 chick embryos. At these stages, expression of Hoxa7 is largely restricted to tail bud neural tube and somitic mesoderm, while Hoxc8, although later expressed in the brachial/thoracic neural tube (Dasen et al., 2005), does not show significant expression in the neural tube (http://geisha.arizona.edu). Although these patterns do not rule out later regulation of Hoxc8 and Hoxa7 through miR-196, only the endogenous neural tube expression of Hoxb8 mRNA was consistent with an early regulatory relationship preceding the onset of neurogenesis.

miR-196-mediated regulation of Hoxb8

Hoxb8 has previously been suggested as a target for miR-196 through bioinformatics and 3'UTR- based luciferase reporter analysis (Yekta et al., 2004). Overexpressed miR-196 was further shown to impair RA- induced expression of Hoxb8 in early chicken limb buds suggesting a "fail safe" post-transcriptional regulatory function for miR-196 (Hornstein et al., 2005). AntagomiR- mediated knockdown of miR-196 in the paraxial mesoderm on the other hand, triggers a posteriorizing transformation of the last cervical vertebra, possibly via derepression of Hoxb8 as well as other putative Hox targets (McGlinn et al., 2009).

In the present study, we have focused on the regulation of Hoxb8 protein levels by miR-196, since the chick Hoxb8 3'UTR has an imperfect seed pairing to miR-196 and hence is predicted to be firstly repressed at the level of translation (Brodersen and Voinnet, 2009; Filipowicz et al., 2008; Nilsen, 2007; Pillai, 2005). According to our data, ectopic expression of miR-196 in the neural tube and CEF cells resulted in efficient down regulation of endogenous Hoxb8. This effect was further mirrored by a GFP reporter bearing the Hoxb8 3'UTR sequence, suggesting a UTR-dependent effect for miR-196. Knock-down of miR-196 in CEFs further resulted in a significant derepression and upregulation of Hoxb8 protein giving miR-196 a potential to achieve a Hoxb8-free caudal neural tube.

In the developing limb, miR-196 appears to represent an additional layer of Hoxb8 regulation, superimposed on preceding regulatory mechanisms operating at the transcriptional level. A primary action via translational repression in chick would argue for a similar role of miR-196 in safeguarding the caudal neural tube from erratic induction of Hoxb8, and/or to assure rapid extinguishment of Hoxb8 protein after miR-196-independent downregulation of its mRNA. However, knockdown of miR-196 concomitant with, or just after downregulation of Hoxb8 mRNA in the caudal neural tube mimics exogenous Hoxb8-triggered inhibition of MN genesis. This observation may rather suggest an involvement of miR-196 in regulating Hoxb8 levels per se, possibly through effects on stability of residual Hoxb8 mRNAs in addition to, or as a result of, sustained translational repression. Indeed, in many instances effective pairing of miRNAs with non-perfectly matching 3'UTR target sites can eventually result in decapping, deadenylation and exonucleolytic degradation of mRNA (Xiao and Rajewsky, 2009).

Spatiotemporal regulation of Hoxb8 and MN specification

The combinatorial action of several Hox proteins with partially overlapping expression domains is implicated in the specification of columnar MN and motor pool identities along the rostro-caudal axis of the neural tube (Dasen et al., 2003; Dasen et al., 2005; Liu et al., 2001; Song and Pfaff, 2005). For instance, the cross-repressive activities of Hoxc6 and Hoxc9 seem to induce LMC and CT columnar identities, respectively, and consolidate the border between brachial and thoracic MNs in apposition to their limb and trunk muscle targets (Dasen et al., 2003). The role of Hox genes in generic motor neuron identities is however, little explored. In this study, deregulated Hoxb8 expression selectively impeded progression of generic MN specification programs towards postmitotic MN fates.

What is the significance of the tightly choreographed spatiotemporal pattern of Hoxb8 activity in the neural tube? The timing of Hoxb8 downregulation, and the concomitant emergence of miR-196 at HH15 coincided with the critical early period of MN specification in the chick caudal neural tube (Matise and Lance-Jones, 1996). The rapid extinguishing of Hoxb8 activity, just prior to the emergence of lumbar $Olig2^+$ pMN progenitors thus indicates a relevance of this pattern for normal caudal MN genesis. Indeed, experimentally sustained Hoxb8 activity appears to selectively block generation of $Isl1/2^+$ postmitotic MNs, without affecting the generation of $Isl1^+$, $Pax2^+$, or $Lim1^+$ ($MNR2/Hb9^-$) interneurons. At the same time, Hoxb8 triggered a significant increase in the number of $Olig2^+BrdU^+pH3^-$ (presumably S-phase) progenitor cells. These data thus indicate that failure of Hoxb8 removal results in an abortive MN generation program, stalling at a

transient pMN progenitor stage prior to MNR2 activation and cell cycle exit. Hoxb8$^+$ cells co-express the markers of early stage precursor motor neurons, Nkx6.1 and Pax6 (Fig. S6A and data not shown), as well as Olig-2 as a marker for further committed MN precursors (Fig. 5 and data not shown). Taken together, these observations suggest that the Hoxb8$^+$ cells maintain the neural fate, progress along the MN generation pathway, but fail to exit the cell cycle and generate mature MNs. Analysis of further neural markers is however necessary to explain the exact nature of these cells and their neurogenic potentials resulting from a probable reprogramming.

We can at present not exclude that the blocking of differentiation could also be achieved by other Hoxb proteins. For instance, a negative control of neural fate specification by Hoxb1 was recently reported (Gouti and Gavalas, 2008). However, the miR196 mediated regulatory mechanism we describe here is specific for Hoxb8, the only Hox gene displaying a mutually exclusive expression pattern at the right time of development. How does Hoxb8 block the eventual acquisition of MN fates in neural progenitors? Outside the neural tube, Hoxb8 gain of function was reported to trigger an increase in the basic proliferative capacity of hematopoietic progenitors (Perkins and Cory, 1993), as well as that of mouse fibroblasts (Aberdam et al., 1991). Could Hoxb8 indirectly affect MN generation through global cell cycle deregulation and/or sustenance? Several observations would argue against such an indirect effect of Hoxb8. For instance, sustained Hoxb8 appears to selectively affect the generation of MNs, but not interneurons, thereby indicating a lineage-specific activity. Moreover, other data suggest that prolonged pMN cycling is not sufficient to impair the eventual expression of postmitotic MN markers (Lobjois et al., 2008). Thus, defects in cell cycle per se do not appear to be sufficient to prevent acquisition of MN identity; it appears there is a more direct effect of Hoxb8 on the induction of immediate pre- and postmitotic MN fate determinants.

In this context, it is notable that the expression of Hoxc9 in the progenitor cells is able to induce preganglionic neurons through downregulation of Hoxc6. Thus, persistent Hoxb8 expression could similarly act by repressing the activity of another more caudally expressed (i.e. 5') Hox gene, which in turn may normally be required for the normal progression of an MN specification program at lumbar levels. Notably, loss of Hoxa10 and Hoxd10 in mice was reported to trigger a decrease in the postmitotic lumbar MN numbers (Lin and Carpenter, 2003). It will therefore be interesting to study the possible regulatory relationships between Hoxb8 and caudally expressed Hox proteins in the normal progression of lumbar MN genesis.

Another question relates to the role of Hoxb8 at more rostral levels, where its expression is maintained following downregulation in the caudal-most neural tube. After initially being broadly expressed, Hoxb8 expression eventually becomes extinguished from the ventro-lateral spinal cord while being maintained in the interneuron-containing dorsal mantle layer (e.g. Fig. 3B). The rapid (apparently miR196-independent) exclusion from the region of eventual MNs generation could thus reflect the general repressive activity of Hoxb8, and may generally entail its downregulation prior to commencement of MN genesis. While this pattern suggests a possible role in interneuron development, overexpression of Hoxb8 affected MN genesis without any apparent compensatory increase in interneuron numbers. Instead, sustained Hoxb8 expression resulted in a selective decrease in MNs, without negatively or positively affecting interneuron numbers, possibly indicating additional roles in later steps of postmitotic interneuron maturation. The extinction of Hoxb8 from the chick HH22 motor columns is an indication that a Hoxb8-free motor column is vital to the timely programming of MNs in later stages. It is therefore a possibility that misexpression of miR-196 in brachial MNs results in an acceleration of motor neuron generation programs, and hence the excessive and/or premature generation of MNs at later stages. In conclusion, the primary target of the regulatory system described in this study is the timing of MN development.

Spatiotemporal microRNA-assisted regulation of generic motor neuron programs

The timed and spatially restricted exclusion of generic cellular programs, such as proliferation and cell cycle exit, appears to be a common theme during organogenesis (Dyer and Cepko, 2001; Li et al., 2002). Similarly, the present study provides evidence for a spatially and temporally restricted regulatory mechanism involved in the normal progression of a generic neuronal subtype program. Rapid downregulation of Hoxb8, at least in part through miR196-mediated repression, facilitates progression of MN differentiation programs in the caudal neural tube. According to collinearity rules, the discrete miR-196 gene position within the Hox cluster therein effectively assures expression that is later and more posterior than its more 3' located target, Hoxb8. In addition to demonstrating a unique requirement for the repression of caudal Hoxb8 activity, which involves microRNA-mediated repression, this study suggests that tightly choreographed spatiotemporal patterns of Hox protein expression may be recruited in a context-dependent manner to shape “generic” neuronal specification programs.

Author contributions

NSA and MK conceived and designed the project and the experiments, and wrote the paper. NSA performed most of the experiments.

Funding

This study was funded by the Max Planck Society.

Competing interests

The authors declare that no competing interests exist.

Acknowledgments

We thank Till Marquardt for his critical and helpful comments and his additional help in setting up and designing some of the experiments. We thank Petra Rus for excellent technical assistance and T. Rosenkranz for useful comments on LNA probe design. We thank Danielle de Jong for critical reading of the manuscript and her helpful comments.

Appendix A. Supplementary data

Supplementary data associated with this article can be found, in the online version, at doi:10.1016/j.ydbio.2010.06.003.

References

Aberdam, D., Negreanu, V., Sachs, L., Blatt, C., 1991. The oncogenic potential of an activated Hox-2.4 homeobox gene in mouse fibroblasts. Mol. Cell. Biol. 11, 554–557.

Bel-Vialar, S., Itasaki, N., Krumlauf, R., 2002. Initiating Hox gene expression: in the early chick neural tube differential sensitivity to FGF and RA signaling subdivides the HoxB genes in two distinct groups. Development 129, 5103–5115.

Brodersen, P., Voinnet, O., 2009. Revisiting the principles of microRNA target recognition and mode of action. Nat. Rev. Mol. Cell Biol. 10, 141–148.

Brown, T., 2001. Analysis of RNA by northern and slot-blot hybridization. Curr. Protoc. Immunol. Chapter 10, Unit 10 12.

Das, R.M., Van Hateren, N.J., Howell, G.R., Farrell, E.R., Bangs, F.K., Porteous, V.C., Manning, E.M., McGrew, M.J., Ohyama, K., Sacco, M.A., Halley, P.A., Sang, H.M., Storey, K.G., Placzek, M., Tickle, C., Nair, V.K., Wilson, S.A., 2006. A robust system for RNA interference in the chicken using a modified microRNA operon. Dev. Biol. 294, 554–563.

Dasen, J.S., Jessell, T.M., 2009. Hox networks and the origins of motor neuron diversity. Curr. Top. Dev. Biol. 88, 169–200.

Dasen, J.S., Liu, J.P., Jessell, T.M., 2003. Motor neuron columnar fate imposed by sequential phases of Hox-c activity. Nature 425, 926–933.

Dasen, J.S., Tice, B.C., Brenner-Morton, S., Jessell, T.M., 2005. A Hox regulatory network establishes motor neuron pool identity and target-muscle connectivity. Cell 123, 477–491.
Dessaud, E., McMahon, A.P., Briscoe, J., 2008. Pattern formation in the vertebrate neural tube: a sonic hedgehog morphogen-regulated transcriptional network. Development 135, 2489–2503.
Duboule, D., 2007. The rise and fall of Hox gene clusters. Development 134, 2549–2560.
Duboule, D., Dolle, P., 1989. The structural and functional organization of the murine HOX gene family resembles that of Drosophila homeotic genes. EMBO J. 8, 1497–1505.
Dyer, M.A., Cepko, C.L., 2001. Regulating proliferation during retinal development. Nat. Rev. Neurosci. 2, 333–342.
Edlund, T., Jessell, T.M., 1999. Progression from extrinsic to intrinsic signaling in cell fate specification: a view from the nervous system. Cell 96, 211–224.
Farh, K.K., Grimson, A., Jan, C., Lewis, B.P., Johnston, W.K., Lim, L.P., Burge, C.B., Bartel, D. P., 2005. The widespread impact of mammalian MicroRNAs on mRNA repression and evolution. Science 310, 1817–1821.
Filipowicz, W., Bhattacharyya, S.N., Sonenberg, N., 2008. Mechanisms of post-transcriptional regulation by microRNAs: are the answers in sight? Nat. Rev. Genet. 9, 102–114.
Gaunt, S.J., 1988. Mouse homeobox gene transcripts occupy different but overlapping domains in embryonic germ layers and organs: a comparison of Hox-3.1 and Hox-1.5. Development 103, 135–144.
Girish, V., Vijayalakshmi, A., 2004. Affordable image analysis using NIH Image/ImageJ. Indian J. Cancer 41, 47.
Glover, J.C., Petursdottir, G., Jansen, J.K., 1986. Fluorescent dextran-amines used as axonal tracers in the nervous system of the chicken embryo. J. Neurosci. Meth. 18, 243–254.
Gouti, M., Gavalas, A., 2008. Hoxb1 controls cell fate specification and proliferative capacity of neural stem and progenitor cells. Stem Cells 26, 1985–1997.
Grimson, A., Farh, K.K., Johnston, W.K., Garrett-Engele, P., Lim, L.P., Bartel, D.P., 2007. MicroRNA targeting specificity in mammals: determinants beyond seed pairing. Mol. Cell 27, 91–105.
Hamburger, V., Hamilton, H.L., 1951. A series of normal stages in the development of the chick embryo. J. Morph. 88, 49–92.
Hornstein, E., Mansfield, J.H., Yekta, S., Hu, J.K., Harfe, B.D., McManus, M.T., Baskerville, S., Bartel, D.P., Tabin, C.J., 2005. The microRNA miR-196 acts upstream of Hoxb8 and Shh in limb development. Nature 438, 671–674.
Iimura, T., Pourquie, O., 2007. Hox genes in time and space during vertebrate body formation. Dev. Growth Differ. 49, 265–275.
Jessell, T.M., 2000. Neuronal specification in the spinal cord: inductive signals and transcriptional codes. Nat. Rev. Genet. 1, 20–29.
Kessel, M., 1994. Hox genes and the identity of motor neurons in the hindbrain. J. Physiol. Paris 88, 105–109.
Kloosterman, W.P., Wienholds, E., de Bruijn, E., Kauppinen, S., Plasterk, R.H., 2006. In situ detection of miRNAs in animal embryos using LNA-modified oligonucleotide probes. Nat. Meth. 3, 27–29.
Krull, C.E., 2004. A primer on using in ovo electroporation to analyze gene function. Dev. Dyn. 229, 433–439.
Landmesser, L.T., 2001. The acquisition of motoneuron subtype identity and motor circuit formation. Int. J. Dev. Neurosci. 19, 175–182.
Lee, S.K., Lee, B., Ruiz, E.C., Pfaff, S.L., 2005. Olig2 and Ngn2 function in opposition to modulate gene expression in motor neuron progenitor cells. Genes Dev. 19, 282–294.
Lee, S.K., Pfaff, S.L., 2001. Transcriptional networks regulating neuronal identity in the developing spinal cord. Nat. Neurosci. 4 (Suppl), 1183–1191.
Li, X., Perissi, V., Liu, F., Rose, D.W., Rosenfeld, M.G., 2002. Tissue-specific regulation of retinal and pituitary precursor cell proliferation. Science 297, 1180–1183.
Lin, A.W., Carpenter, E.M., 2003. Hoxa10 and Hoxd10 coordinately regulate lumbar motor neuron patterning. J. Neurobiol. 56, 328–337.
Liu, J.P., Laufer, E., Jessell, T.M., 2001. Assigning the positional identity of spinal motor neurons: rostrocaudal patterning of Hox-c expression by FGFs, Gdf11, and retinoids. Neuron 32, 997–1012.
Lobjois, V., Bel-Vialar, S., Trousse, F., Pituello, F., 2008. Forcing neural progenitor cells to cycle is insufficient to alter cell-fate decision and timing of neuronal differentiation in the spinal cord. Neural Develop. 3, 4.
Mansfield, J.H., Harfe, B.D., Nissen, R., Obenauer, J., Srineel, J., Chaudhuri, A., Farzan-Kashani, R., Zuker, M., Pasquinelli, A.E., Ruvkun, G., Sharp, P.A., Tabin, C.J., McManus, M.T., 2004. MicroRNA-responsive 'sensor' transgenes uncover Hox-like and other developmentally regulated patterns of vertebrate microRNA expression. Nat. Genet. 36, 1079–1083.
Marquardt, T., Pfaff, S.L., 2001. Cracking the transcriptional code for cell specification in the neural tube. Cell 106, 651–654.
Matise, M.P., Lance-Jones, C., 1996. A critical period for the specification of motor pools in the chick lumbosacral spinal cord. Development 122, 659–669.
McGlinn, E., Yekta, S., Mansfield, J.H., Soutschek, J., Bartel, D.P., Tabin, C.J., 2009. In ovo application of antagomiRs indicates a role for miR-196 in patterning the chick axial skeleton through Hox gene regulation. Proc. Natl. Acad. Sci. U. S. A. 106, 18610–18615.
Mizuguchi, R., Sugimori, M., Takebayashi, H., Kosako, H., Nagao, M., Yoshida, S., Nabeshima, Y., Shimamura, K., Nakafuku, M., 2001. Combinatorial roles of olig2 and neurogenin2 in the coordinated induction of pan-neuronal and subtype-specific properties of motoneurons. Neuron 31, 757–771.
Nilsen, T.W., 2007. Mechanisms of microRNA-mediated gene regulation in animal cells. Trends Genet. 23, 243–249.
Novitch, B.G., Chen, A.I., Jessell, T.M., 2001. Coordinate regulation of motor neuron subtype identity and pan-neuronal properties by the bHLH repressor Olig2. Neuron 31, 773–789.
Ohler, U., Yekta, S., Lim, L.P., Bartel, D.P., Burge, C.B., 2004. Patterns of flanking sequence conservation and a characteristic upstream motif for microRNA gene identification. RNA 10, 1309–1322.
Pearson, J.C., Lemons, D., McGinnis, W., 2005. Modulating Hox gene functions during animal body patterning. Nat. Rev. Genet. 6, 893–904.
Perkins, A.C., Cory, S., 1993. Conditional immortalization of mouse myelomonocytic, megakaryocytic and mast cell progenitors by the Hox-2.4 homeobox gene. EMBO J. 12, 3835–3846.
Pillai, R.S., 2005. MicroRNA function: multiple mechanisms for a tiny RNA? RNA 11, 1753–1761.
Price, S.R., Briscoe, J., 2004. The generation and diversification of spinal motor neurons: signals and responses. Mech. Dev. 121, 1103–1115.
Rinn, J.L., Kertesz, M., Wang, J.K., Squazzo, S.L., Xu, X., Brugmann, S.A., Goodnough, L.H., Helms, J.A., Farnham, P.J., Segal, E., Chang, H.Y., 2007. Functional demarcation of active and silent chromatin domains in human HOX loci by noncoding RNAs. Cell 129, 1311–1323.
Rowitch, D.H., Lu, Q.R., Kessaris, N., Richardson, W.D., 2002. An 'oligarchy' rules neural development. Trends Neurosci. 25, 417–422.
Sehm, T., Sachse, C., Frenzel, C., Echeverri, K., 2009. miR-196 is an essential early-stage regulator of tail regeneration, upstream of key spinal cord patterning events. Dev. Biol. 334, 468–480.
Sessa, L., Breiling, A., Lavorgna, G., Silvestri, L., Casari, G., Orlando, V., 2007. Noncoding RNA synthesis and loss of Polycomb group repression accompanies the colinear activation of the human HOXA cluster. RNA 13, 223–239.
Sharma, K., Sheng, H.Z., Lettieri, K., Li, H., Karavanov, A., Potter, S., Westphal, H., Pfaff, S. L., 1998. LIM homeodomain factors Lhx3 and Lhx4 assign subtype identities for motor neurons. Cell 95, 817–828.
Song, M.R., Pfaff, S.L., 2005. Hox genes: the instructors working at motor pools. Cell 123, 363–365.
Sur, M., Rubenstein, J.L., 2005. Patterning and plasticity of the cerebral cortex. Science 310, 805–810.
Tanabe, Y., Jessell, T.M., 1996. Diversity and pattern in the developing spinal cord. Science 274, 1115–1123.
Tanabe, Y., William, C., Jessell, T.M., 1998. Specification of motor neuron identity by the MNR2 homeodomain protein. Cell 95, 67–80.
Tarui, T., Takahashi, T., Nowakowski, R.S., Hayes, N.L., Bhide, P.G., Caviness, V.S., 2005. Overexpression of p27 Kip 1, probability of cell cycle exit, and laminar destination of neocortical neurons. Cereb. Cortex 15, 1343–1355.
William, C.M., Tanabe, Y., Jessell, T.M., 2003. Regulation of motor neuron subtype identity by repressor activity of Mnx class homeodomain proteins. Development 130, 1523–1536.
Xiao, C., Rajewsky, K., 2009. MicroRNA control in the immune system: basic principles. Cell 136, 26–36.
Yekta, S., Shih, I.H., Bartel, D.P., 2004. MicroRNA-directed cleavage of HOXB8 mRNA. Science 304, 594–596.
Yekta, S., Tabin, C.J., Bartel, D.P., 2008. MicroRNAs in the Hox network: an apparent link to posterior prevalence. Nat. Rev. Genet. 9, 789–796.